Heliyon 8 (2022) e09129

Contents lists available at ScienceDirect

Heliyon

journal homepage: www.cell.com/heliyon

Research article

# Predicting the strength of concrete made with stone dust and nylon fiber using artificial neural network

Sourav Ray *, Mohaiminul Haque, Tanvir Ahmed, Ayesha Ferdous Mita, Md Hadiuzzaman Saikat, Md Mafus Alom

*Department of Civil and Environmental Engineering, Shahjalal University of Science and Technology, Sylhet, Bangladesh*

ARTICLE INFO

*Keywords:*
Stone dust
Nylon fiber
Compressive strength
Splitting tensile strength
Artificial neural network

ABSTRACT

Excessive demand of concrete is causing depletion of natural sand resources. Especially, the extraction of river sand negatively affects its surrounding environment. A sustainable solution to this problem can be the proper utilization of waste materials and by-products like stone dust (SD) as fine aggregate replacement in concrete. The recycling of stone dust as a construction material lessens the use of natural resources and helps to solve landfill scarcity as well as environmental problems. Addition of nylon fiber (NF) as fiber reinforcement can also attribute to enhance the properties of concrete. This research aims at utilizing SD as fine aggregate along with NF, and assessing the compressive strength and splitting tensile strength of concrete. Although the individual effects of incorporating stone dust and nylon fiber in concrete have been investigated in previous researches, their combined effects, as well as effects of water cement (WC) ratio on concrete strength, have not been studied yet. In this study, volumetric percentages of stone dust (20%–50%) and nylon fiber (0.25%–0.75%) and three different water cement ratio (0.45, 0.50 and 0.55) have been considered as three independent variables to develop probabilistic models for compressive strength and splitting tensile strength of concrete using artificial neural network (ANN). The values of coefficient of determination ($R^2$) and other statistical parameters of the developed probabilistic models indicate the accuracy of the models to predict the concrete strength. In terms of compressive strength at early age, the optimal percentages of SD and NF have been found as 20% and 0.25%, respectively. However, the strength gradually drops as water cement ratio elevates from 0.45 to 0.55. The reduction of the splitting tensile strength has been observed for increasing SD from 20% to 50%, whereas, strength increases for rising NF and WC up to mid-level.

## 1. Introduction

Concrete has appeared as the prevailing construction material for all types of infrastructure of the twenty-first century due to its longevity, durability, easy preparation and fabrication from readily available constituents (Aggarwal et al., 2007; Ray et al., 2021c). It is the second most consumed material after water. Every year, over 10 billion tons of concrete is produced which represents nearly 1.5 ton per capita in the world (Kanojia and Jain, 2017). The production of one cubic meter of concrete requires nearly equal volume of aggregates (Gupta et al., 2021). In concrete, aggregates occupy 70–80% in which 25–30% is filled by fine aggregate (Kanojia and Jain, 2017). Since fine aggregate comes from natural sources, its excessive demand has resulted in a shortage of resources. In addition, the widespread reduction of sand sources causes negative impacts on associate ecosystem, landscape, water tables and riverbeds (Ray et al., 2021a).

On the other hand, due to high production, construction and demolitions activities in developing countries, waste generation is on rise and has become a matter of grave concern. The appalling status of virgin land is growing as a result of an increase in the percentage of dumping by abandoned waste materials including stone dust (SD) raising social, global, and environmental concerns (Bisht and Ramana, 2018; Ray et al., 2021d). Stone dust is obtained at crusher plants as rubbish where the artificial crushing of rock or gravels is done to obtain coarse aggregate (Figure 1). At present, this waste is not recycled in any form except for dumping in landfills (Ahmed et al., 2010; Ray et al., 2021b). During crushing, handling and disposal, this waste disperses a great extent of fine solid particles in air, water and soil as pollutant (Galetakis and Soultana, 2016). These, scarcity of resources and problems associated

* Corresponding author.
*E-mail addresses:* sourav.ceesust@gmail.com, sourav-cee@sust.edu (S. Ray).

https://doi.org/10.1016/j.heliyon.2022.e09129
Received 8 September 2021; Received in revised form 13 December 2021; Accepted 14 March 2022

**Figure 1.** Stone dust as by-product of stone crushing.

with wastes, motivate researchers to use stone dust in concrete production without reducing quality and hardened strength of concrete. Utilization of stone dust provides homogeneous mix to concrete and can enhance compressive, splitting tensile and flexural strength of concrete since previous researches appeared to suggest a promising option as construction material (Gadgihalli et al., 2017; Gupta et al., 2021; Hameed and Sekar, 2009; Mundra et al., 2016; Syed and Quadri, 2013).

Stone dust is such a promising waste to be mentioned with high specific gravity, almost similar particle sizes that make it potential for use as fine aggregate in concrete (Reddy et al., 2015). However, stone dust has little lower value of fineness modulus compared to natural sand (Suman and Srivastava, 2015). Worldwide, stone businesses create 68 million tons of processed products annually causing disposal problems, makes an incredible issue for transfer and environmental hazards (Prakash and Rao, 2016). As for Bangladesh, about 100000 cubic feet of stone dust is produced during stone crushing (Muhit et al., 2014). The utilization of crushed stone dust in making concrete and mortar not only preclude the decline of sources of natural sand but also solves the issues associated with disposal and environmental of this dust (Rajput, 2018). Syed and Quadri (2013) and Turuallo et al. (2020), Yadav (2021) found that maximum compressive strength was obtained about 40% replacement of sand with crushed dust. The concrete specimens tested by Singh et al. (2016) was found rising the strength up to 30% addition of stone dust. Kala and Sethuraman (2013) studied the effect of stone dust varying from 25% to 100% on the compressive strength of concrete and found that highest strength occurred at 25%. Similar results were stated by Arivumangai (2014) where replacement level higher than 25% underwent a drop of the strength. Oyekan and Kamiyo (2008) also noticed that stone dust can be used up to 15% of river sand. However, for incorporation of stone dust, Serelis et al. (2018) reported decrement in the strength lower than control concrete. In addition, no significant influence on the compressive strength was found by Vijayalakshmi et al. (2013) for replacement of stone dust from 0%-15%.

Meanwhile, in case of splitting tensile strength, Rao (2021) focused on the behaviour of concrete having stone dust and promulgated that tensile strength increases significantly for rising incorporation of the dust. The experimental outcomes of the research of Alok et al. (2020), and Prasanth et al. (2020) revealed that the strength increased with the elaboration of stone dust's percentage up to 40%. Moreover, rising trend of the strength of concrete was observed by Khan et al. (2018) and Vijayalakshmi et al. (2013) for inclusion of stone dust and found optimum strength at 15% substitution of river sand with the dust. To increase the usage (%) of SD in concrete without compromising the strength of concrete fiber reinforcement can be a good solution.

Fiber reinforced concrete (FRC) is becoming popular due to its promising performance in structural reliability (Verma, 2016). Fiber improves flexural strength, splitting tensile strength, freeze-thaw resistance, toughness, resistance to fatigue, etc. (Choi et al., 2011; Gadgihalli et al., 2017; Haque et al., 2021). It also reduces swelling of micro and macro crack, segregation and bleed-water (Wang and Shah, 2001). Extensive investigation on FRC has established that the addition of different types of fiber such as steel, glass, synthetic, and carbon improves strength, toughness, ductility, post-cracking resistance and resist localize tension that causes cracking. Nylon fiber (NF) is such a well-known material used as fiber reinforcement in concrete. The reason for using nylon fiber is that it has good hardness, resilience, and durability, resistant to soil and dirt, has good abrasion and wearing characteristics, cost effects, availability in different cross section and color (Swami and Gupta, 2016). Gadgihalli et al. (2017) promulgated that nylon fiber, as admixture, can increase the compressive strength about 4.18% and 1.77% for M20 and M30 grade respectively compared to conventional concrete. Likewise, Munadrah et al. (2021) examined the effect of 0.5% and 1% inclusion of nylon fiber and noticed increment of compressive strength by 68.75% and 126.26% respectively compared to control concrete. Ahmad et al. (2021) added 2%–8% nylon fiber in interval of 2% and found that the highest compressive strength happened at 5.5%. An increasing pattern was observed by Vaishnavi et al. (2019) when proportion of nylon fiber rose from 0.125% to 0.300%. On the other hand, concrete made of 1.5% nylon fiber augment significant splitting tensile strength in comparison with conventional concrete (Zul et al., 2021). In addition, Lashari et al. (2021) reported gradual increment of the strength since nylon fiber increases up to 0.5% in step of 0.1%. Moreover, Bheel et al. (2021) found 1% nylon fiber to be optimum percentage providing maximum splitting tensile strength that was 14.1% more that concrete having no nylon fiber.

The improvement of strength in concrete is determined by water cement ratio and the bond at the contact surface of hydrated binding (cement) paste and its constituents. For fluidity of concrete mixture having 0.80 water cement ratio is immense enough to induce collapse of the concrete cone resulting in reduction of strength of concrete (Alawode and Idowu, 2011). While, decrease in w/c positively affect concrete by developing strengths (Anifowose et al., 2021). Singh et al. (2015) found 0.5 water cement ratio, within the range of 0.5–1.2 water cement ratio, as the point where maximum compressive and splitting tensile strength happened. Moreover, Yaşar et al. (2004) stated that 20% compressive strength of concrete was attributed to optimum water cement ratio (0.33–0.36) at 28-day curing time. However, low or medium water cement ratio may not develop the strength since stone dust has low fineness modulus than river sand implying that stone dust would use more cement paste resulting in less fluidity of the concrete mix (Dhir et al., 2017). An optimum water cement ratio could be a feasible approach to get the best concrete (Anifowose et al., 2021). Hence, in this study, three different water cement ratios (0.45–0.55) have been used to understand the performances along with other materials.

Hence, a correlation between affecting factors (stone dust, nylon fiber and water cement ratio) and influenced factors (compressive strength and splitting tensile strength) needs to be created to investigate the influences of these input variables on the output variables. Over the past few decades, application of computer models to investigate the resulting outcome of concrete mixes has received ample priority. One mentionable method is artificial neural networks (ANN) which emulate the processing system of biological neuron, have structure of vast parallel, interconnected, unvarnished computing constituents called neurons arranged in layers (Alshihri et al., 2009; O. Akande et al., 2014). ANN has the potentiality of solving convoluted problems owing to nonlinear processing, parallel processing systems (Ozturan et al., 2008; Stathakis, 2009). Topçu and Saridemir (2007) employed ANN in predicting the concrete properties made of waste aggregate. Kewalramani and Gupta (2006) simulated compressive strength of concrete using artificial neural networks. Mashhadban et al. (2016) constructed ANN models to simulate

mechanical properties of fiber-reinforced concrete. The effect of silica fume and fly ash on the compressive strength of concrete was assessed by Shariati et al. (2021). In another study of the author, artificial neural network-genetic algorithm (ANN-GA) was employed to simulate the strength of concrete containing furnace slag and fly ash (Shariati et al., 2020b).

Previous researchers have studied the effect of stone dust and nylon fiber in concrete individually. So, the present study is aimed to find the effects of stone dust (SD), nylon fiber (NF), and water cement (WC) ratio combinedly on the compressive and splitting tensile strength of concrete from the ANN-based models. Also, the prediction of the properties of concrete using artificial neural networks is unique compared to earlier research. Feedforward Neural Networks methods were adopted for the development of ANN models where SD, NF, and WC were taken as input factors and 7-day and 28-day compressive and splitting tensile strength were taken as responses.

## 2. Experimental study

### 2.1. Material properties

Portland Limestone Cement (PLC) as binding material has been used having 27% normal consistency. The initial and final setting time of PLC was found 130 and 170 min respectively. In this present study, 20 mm and 10 mm downgrade crushed stone chips as coarse aggregate with ratio of 7:3 respectively was adopted. As fine aggregate, river sand having 4.75 mm maximum size and 2.6 fineness modulus has been utilized. Stone dust that was amassed from a local crusher plant was taken as partial replacement of natural fine aggregate having size varied between 0.15 mm to 4.75 mm (Figure 2). The particle size distribution curve of river sand and stone dust has been displayed in Figure 3. The nylon as fiber reinforcement was collected from a local market which is normally used for fishing nets. Nylon has been processed manually into laboratory to make fiber of 20 mm length (Figure 4). Table 1 depicts the physical properties used material.

### 2.2. Mixture proportioning

The relative proportions of constituents used in preparation of test specimens for testing of hardened properties of concrete are given in Table 2. A total of 13 concrete mixes were used with the same mix ratio of 1:1.5:3 but having different types of water cement ratio. In each of the proportions, stone dust was used as 20%, 35%, and 50% in place of fine aggregate while the addition of nylon fiber was ranged from 0.25% to 0.75%. Volumetric percentages of all variables that have been employed in this research are presented in Table 3.

### 2.3. Preparation of specimens

All concrete specimens were cast using molds of 100 mm diameter and 200 mm height for hardened strength tests. Molds were coated with grease followed by casting and drying of specimens for 24 h into a constant room temperature. Then the concrete was removed from the molds and immediately submerged in fresh clean water. Specimens for compressive and splitting tensile strength tests were cured for 7 and 28 days. Test of sieve analysis, bulk density, flakiness and elongation, specific gravity of coarse aggregate and fine aggregate, compressive strength and splitting tensile strength were executed in accordance with ASTM C136, C29, D-4719, C127, C128, C39 and C496 respectively.

### 2.4. Artificial neural network

ANN simulates the functioning of the biological nervous system that is made of small units called neurons. An input layer, one or more hidden layers, and an output layer are used to organize neurons (Figure 5) (Dantas et al., 2013; Gupta et al., 2019; Ray et al., 2021a; Shariati et al., 2020a). The ANN shown in Figure 5 is called feed-forward network where computations proceed along the forward direction only.

ANN is formed of inputs, weights, sum function, activation function and outputs (Figure 6). Inputs are information from external world that are used by neurons to learn and recognize the process. A neuron can have several inputs but one output. The input layer contains one neuron for each of the input variables. Each input has a coefficient referred weight assigned to it. Sum function calculates the net input that comes to a cell. Activation function (sigmoid function) calculates the outcome of the cell by processing the total input gained from sum function. In multilayer network, the output of one layer constitutes the input to the next layer. The output obtained from the output neurons constitutes the network output (Khan et al., 2021). Neuron functions as follows: the neuron's inputs are multiplied by the associated weights. The outcome (dimensionless) is then added together using Eq. (1) (Topçu and Saridemir, 2007).

$$x = \left( \sum_{i=1}^{n} w_i y_i + b \right) \tag{1}$$

where, $x$ is the outcome of the neuron, $y_i$ *is* the input value, $w_i$ *is* the associated weight, $b$ is the bias value and $\sum$ is sum function. The output of the neuron is applied to a sigmoid function to form net output (dimensionless) of the neuron by employing Eq. (2) (Bonagura and Nobile, 2021) where α is a constant.

$$Net\ output = f(z) = \frac{1}{1 + e^{-\alpha x}} \tag{2}$$

Initially, the values of weights and bias are randomly chosen and afterward resolved by the training processes. There are numerous processes available including back propagation (BP) and cascade correlation (CC) schemes. Back-propagation learning is an iterative process that adapts the weights from the output layer to the input layer. Any learning algorithm's focus is to reduce the mean square error (MSE) between simulated and experimental outcomes (in the training sample) while preserving the networks' generality. The performance of the network (generality) is evaluated by a testing data set. Validation set is used to train the network to discover and maximize the best system to address a specific issue. (Alshihri et al., 2009).

### 2.5. Model assessment

To examine the accuracy of the developed ANN models for 7-day and 28-day compressive and splitting tensile strength coefficient of correlation (Hammoudi et al., 2019), coefficient of determination (Ray et al., 2021e), mean square error (Duan et al., 2013), and coefficient of efficiency (Grunwald and Frede, 1999), mean absolute error (Maran, 2013), average error (Getahun et al., 2018) were employed. The corresponding equations, shown as Eqs. (3), (4), (5), (6), (7), and (8) of these tools are given below.

**Figure 2.** Stone dust.

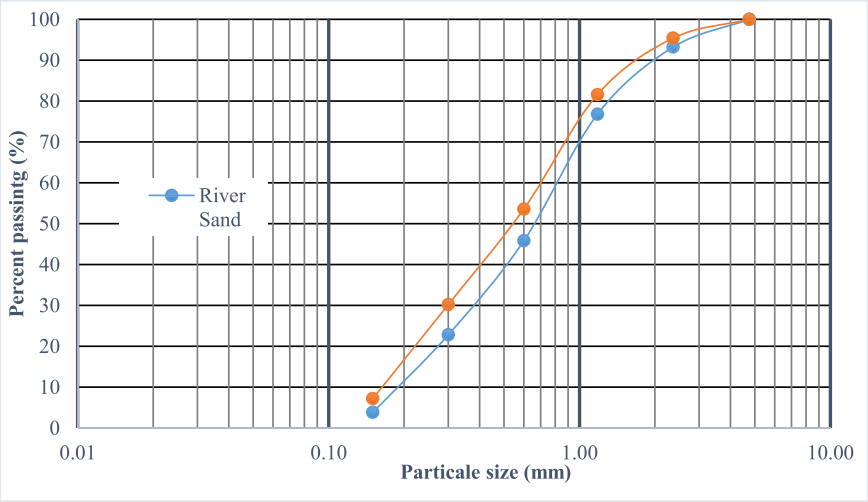


**Figure 3.** Particle size distribution of river sand and stone dust.

**Figure 4.** Nylon fiber.

**Table 1.** Properties of aggregates.

| Name of property | FA | SD | CA |
|---|---|---|---|
| Specific gravity | 2.74 | 2.11 | - |
| Density (kg/m$^3$) | 1600 | 1430 | - |
| Water absorption capacity (%) | 2.24 | 3.3 | 1.01 |
| Coefficient of uniformity | 3.96 | 3.83 | |
| Coefficient of gradation | 0.89 | 0.77 | |
| Fineness modulus | 2.67 | 2.54 | |
| Flakiness (%) | - | - | 17.8 |
| Elongation (%) | - | - | 35.29 |

FA = Fine aggregate, SD = Stone dust, CA = Coarse aggregate.

$$\text{Coefficient of determination } (R) = \frac{\sum_1^n (a_i - \bar{a})(p_i - \bar{p})}{\sqrt{\sum_1^n (a_i - \bar{a})^2 \sum_1^n (p_i - \bar{p})^2}} \quad (3)$$

$$\text{Coefficient of determination } (R^2) = \left( \frac{\sum_1^n (a_i - \bar{a})(p_i - \bar{p})}{\sqrt{\sum_1^n (a_i - \bar{a})^2 \sum_1^n (p_i - \bar{p})^2}} \right)^2 \quad (4)$$

$$\text{Mean square error } (MSE) = \frac{\sum_1^n (p_i - a_i)^2}{N} \quad (5)$$

$$\text{Coefficient of efficiency } (E_f) = \frac{\sum_1^n (a_i - \bar{a})^2 - \sum_1^n (p_i - a_i)^2}{\sum_1^n (a_i - \bar{a})^2} \quad (6)$$

$$\text{Mean absolute error } (MAE) = \frac{1}{N} \sum_1^N |p_i - a_i| \quad (7)$$

$$\text{Average error } (AE) = \frac{1}{N} \sum_1^n (p_i - a_i) \quad (8)$$

Here, $a_i$ is actual data, $p_i$ is predicted data, $\bar{a}$ and $\bar{p}$ are the average of actual and predicted data respectively and $N$ is the number of samples. The all mentioned statistical parameters in the present study have no unit.

## 3. Results and discussions

### 3.1. ANN model evaluation

In order to confirm the suitability of the developed ANN models for 7 and 28 days compressive and splitting tensile strength, the experimental values of each experiment were weighed to corresponding predicted values as can be seen in Figures 7, 8, 9, and 10. These figures show the significance of the ANN regression models since predicted data were close to experimental data (Ray et al., 2021a). The figures also represent the best fit line, which is defined by the best linear function (y = mx + c) and has an elevated coefficient of determination (Nazerian et al., 2018).

The correlation coefficient (R) of the set of training, validation, testing and overall for each model are presented in Table 4. These R (overall) values close to 0.9 hint at a good degree of relation between the predicted and actual values in all cases (Schober and Schwarte, 2018). From Table 4, the R-value in the testing set was 0.89 and 0.94 for compressive strength at 7 and 28 days respectively, which implies that the constructed model can interpret at least 90% of the estimated data. Almost similar outcomes were noticed for splitting tensile strength for both ages which confirm the applicability of ANN approaches for accurate prediction in this study (Demirkir et al., 2013). The constructed models are good fit since coefficient of determination ($R^2$) values of the models were above 0.8 (Hassan et al., 2020).

The ANN model of compressive and splitting tensile strength at 7 and 28 days simulated the actual results with MSE values of 0.04441, 0.09581, 0.00508 and 0.01783 respectively which implies that residual errors were not considerable (Table 5). In comparison of predicted results with actual values, the 7-day compressive strength and splitting tensile strength values were overpredicted on average values of 0.04477 and 0.01329 respectively, whereas, for 28 days, the simulation was 0.09063 less for compressive strength and 0.02753 less for splitting tensile

**Table 2.** Concrete mix proportions.

| Mix Number | Water Cement ratio | Cement (kg/m$^3$) | Water (kg/m$^3$) | Coarse Aggregate (kg/m$^3$) | Fine Aggregate | | | Nylon Fiber | |
|---|---|---|---|---|---|---|---|---|---|
| | | | | | River Sand | Stone Dust | | % | kg/m$^3$ |
| | | | | | kg/m$^3$ | % | kg/m$^3$ | | |
| M1 | 0.45 | 400.00 | 180.00 | 1200.00 | 390.00 | 35.00 | 210.00 | 0.25 | 6.00 |
| M2 | 0.45 | 400.00 | 180.00 | 1200.00 | 480.00 | 20.00 | 120.00 | 0.50 | 12.00 |
| M3 | 0.45 | 400.00 | 180.00 | 1200.00 | 300.00 | 50.00 | 300.00 | 0.50 | 12.00 |
| M4 | 0.45 | 400.00 | 180.00 | 1200.00 | 390.00 | 35.00 | 210.00 | 0.75 | 18.00 |
| M5 | 0.50 | 400.00 | 200.00 | 1200.00 | 480.00 | 20.00 | 120.00 | 0.25 | 6.00 |
| M6 | 0.50 | 400.00 | 200.00 | 1200.00 | 300.00 | 50.00 | 300.00 | 0.25 | 6.00 |
| M7 | 0.50 | 400.00 | 200.00 | 1200.00 | 480.00 | 20.00 | 120.00 | 0.75 | 18.00 |
| M8 | 0.50 | 400.00 | 200.00 | 1200.00 | 300.00 | 50.00 | 300.00 | 0.75 | 18.00 |
| M9 | 0.55 | 400.00 | 220.00 | 1200.00 | 390.00 | 35.00 | 210.00 | 0.25 | 6.00 |
| M10 | 0.55 | 400.00 | 220.00 | 1200.00 | 480.00 | 20.00 | 120.00 | 0.50 | 12.00 |
| M11 | 0.55 | 400.00 | 220.00 | 1200.00 | 300.00 | 50.00 | 300.00 | 0.50 | 12.00 |
| M12 | 0.55 | 400.00 | 220.00 | 1200.00 | 390.00 | 35.00 | 210.00 | 0.75 | 18.00 |
| M13 | 0.50 | 400.00 | 220.00 | 1200.00 | 390.00 | 35.00 | 210.00 | 0.50 | 12.00 |

**Table 3.** Proportions of variables.

| Variable | Percentages | | |
|---|---|---|---|
| | Low Level | Intermediate Level | High Level |
| SD% | 20 | 35 | 50 |
| NF% | 0.25 | 0.50 | 0.75 |
| WC | 0.45 | 0.50 | 0.55 |

WC = Water cement ratio.

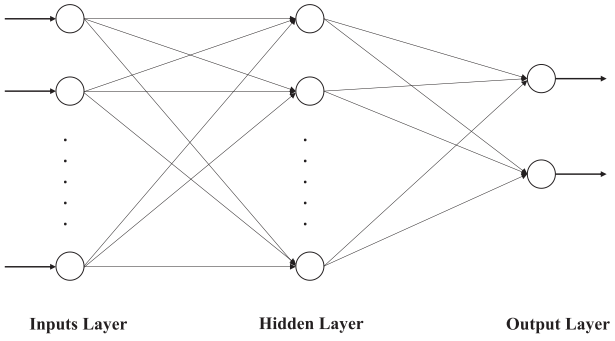


**Figure 5.** Structure of ANN.

strength. MAE demonstrates that deviation of the predicted values of 7 and 28 days compressive and splitting tensile strength values happened by 0.12986, 0.20341, 0.05715 and 0.11669 respectively from experimentally determined results. These validate that the models were fit for precise simulation of the hardened strength of concrete (Getahun et al., 2018). Measures of coefficient of efficiency ($E_f$) close to 1 implies good fitness between actual and predicted data (Grunwald and Frede, 1999).

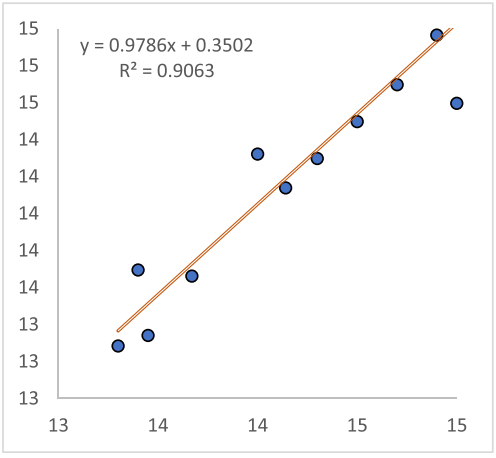


**Figure 7.** Correlation coefficient for 7 days compressive strength.

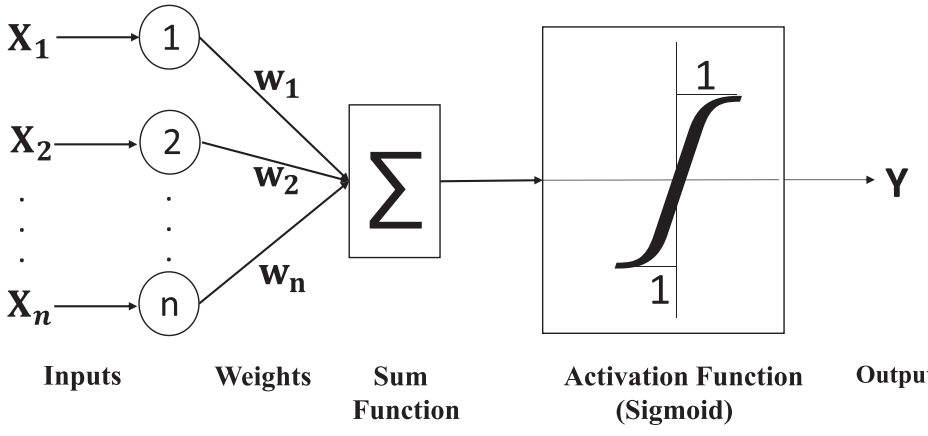


**Figure 6.** A simple neuron model.

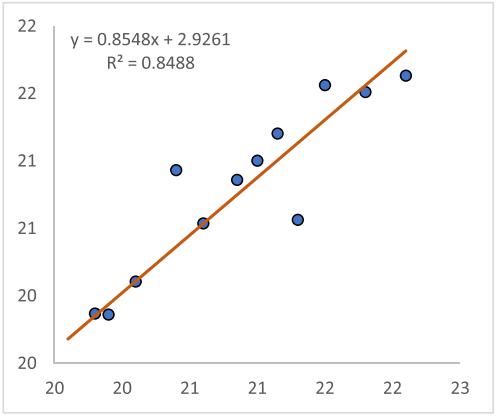


**Figure 8.** Correlation coefficient for 28 days compressive strength.

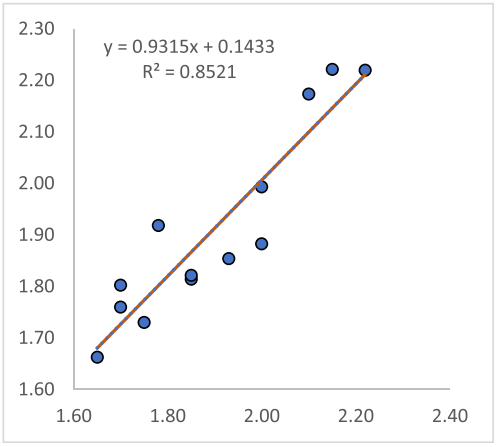


**Figure 9.** Correlation coefficient for 7 days splitting tensile strength.

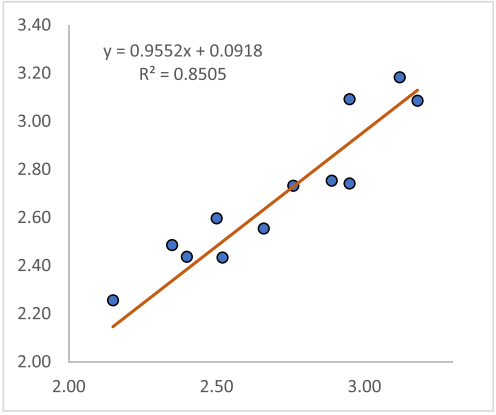


**Figure 10.** Correlation coefficient for 28 days splitting tensile strength.

**Table 4.** Coefficient of Correlation of ANN models.

| Test type | Training | Validation | Testing | Overall |
|---|---|---|---|---|
| CS-7 | 0.99998 | 0.97828 | 0.88727 | 0.95199 |
| CS-28 | 0.98669 | 0.92553 | 0.93670 | 0.92129 |
| STS-7 | 0.92099 | 0.96908 | 0.87200 | 0.92308 |
| STS-28 | 0.96564 | 0.97468 | 0.99350 | 0.92221 |

**Table 5.** Parameter of ANN models.

| Tool | C7 | C28 | S7 | S28 |
|---|---|---|---|---|
| R | 0.95199 | 0.92129 | 0.92308 | 0.92221 |
| $R^2$ | 0.90628 | 0.84878 | 0.85207 | 0.85048 |
| MSE | 0.04441 | 0.09581 | 0.00508 | 0.01783 |
| MAE | 0.12986 | 0.20341 | 0.05715 | 0.11669 |
| AE | 0.04477 | -0.09063 | 0.01329 | -0.02753 |
| $E_f$ | 0.90234 | 0.96848 | 0.83906 | 0.83036 |

### 3.2. Response surface of ANN models

#### 3.2.1. Compressive strength

To develop the correlations between the responses and the process parameters, it is necessary to study the influence of each parameter on the strength. For this, in the present study, 3D response surface plots (Figures 11, 12, 13, 14, 15, 16, 17, 18, 19, 20, 21, and 22) for the compressive and splitting tensile strength at 7 and 28 days were developed using JMP software by providing predicted values with matrices of the input variables. In Figure 11, compressive strength dropped from 15.2 MPa to 13.28 MPa with the increasing SD up to 35%. One of the causes for the lowering in compressive strength was the larger surface area of SD aggregate particles (Joel, 2010; Singh et al., 2016). Further increase of the dust resulted in rise of the strength. This increase was attributed by Rao et al. (2012) to rough and irregular granite particles, high frictional resistance of SD. According to the plot, 20% SD with 0.25–0.75% NF showed higher strength compared with other proportions of SD and NF. Similar tendency can be seen in case of NF where the maximum result occurred at initial level at 14.6 MPa. The 3D figure showed that as the NF increases to 0.5%, the compressive strength decreases and could be attributed to the contribution of pores from the high proportion of NF (Abbas et al., 2002; Ismail et al., 2020; Lee et al., 2012).

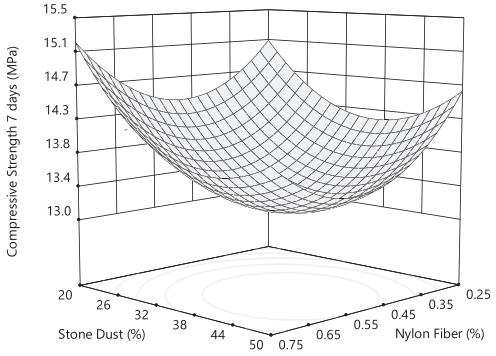


**Figure 11.** Response surface of 7 days compressive strength against stone dust and nylon fiber.

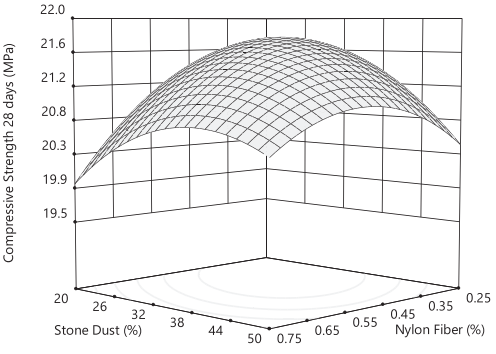


**Figure 12.** Response surface of 28 days compressive strength against stone dust and nylon fiber.

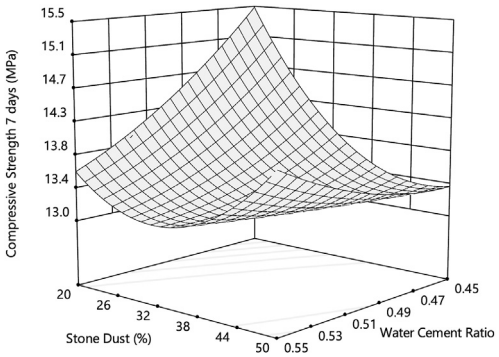


**Figure 13.** Response surface of 7 days compressive strength against stone dust and water cement ratio.

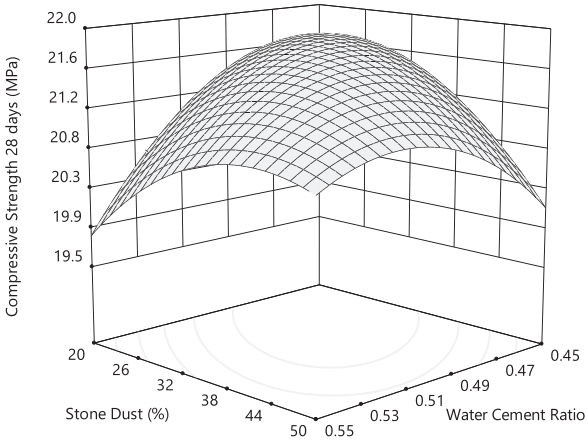


**Figure 14.** Response surface of 28 days compressive strength against stone dust and water cement ratio.

However, additional increment of NF causes an increment of strength which is consistent with the study presented by Bheel et al. (2021) and Munadrah et al. (2021). This augmentation of the strength might be happened by the NF's controlling of the formation and widening of cracks (Bheel et al., 2021).

Figure 15, when NF varies from 0.25%-0.50% and WC range from 0.45-0.55 at fixed SD of 35%, indicated that increment of WC within the specified range caused decrement of compressive strength. This trend is in line with the result reported by Joshi and Dave (2016), Schulze (1999), Yaşar et al. (2004). The addition level of 0.75% NF with 0.45 WC appeared to be the peak strength displayed in the plot. A similar decreasing pattern of the strength with the rising WC can be seen in

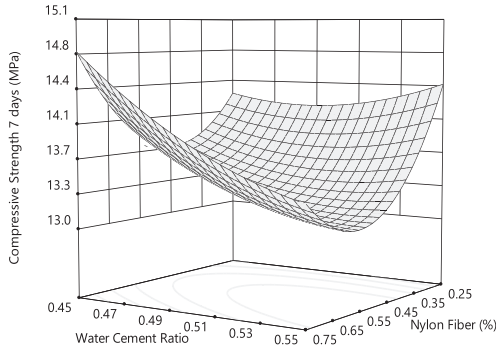


**Figure 15.** Response surface of 7 days compressive strength against water cement ratio and nylon fiber.

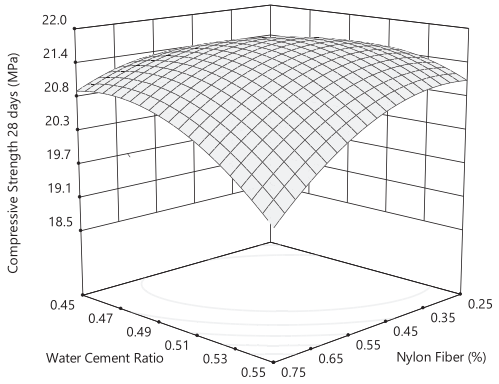


**Figure 16.** Response surface of 28 days compressive strength against water cement ratio and nylon fiber.

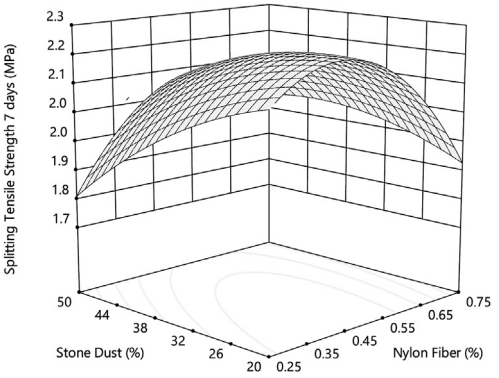


**Figure 17.** Response surface of 7 days splitting tensile strength against stone dust and nylon fiber.

Figure 13. According to the 3D plot, peak strength of 15.56 MPa occurred in the region of 20% SD and 0.45 WC ratio.

Figure 12 represents the 3D surface plot of 28 days compressive strength as a function of SD and NF, while WC was kept constant at 0.50. It was seen that the strength rose from 19.87 to 21.2 MPa when the SD was changed from 20% to 35%. Divakar et al. (2012) and Srivastava et al. (2014) divulged an identical pattern of outcomes in their research. When the proportion of SD was higher than 35%, the compressive strength decreased. This drop of strength could be attributed to supplement SD after filling voids inside concrete (Verma et al., 2020).

As illustrated in Figure 14, indicated that the influence of WC ratio on the compressive strength of concrete is most significant when the ratio is

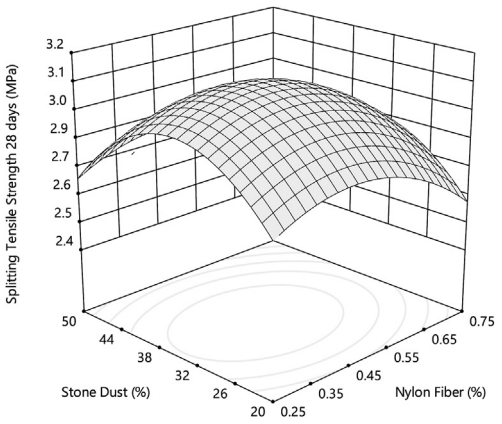


**Figure 18.** Response surface of 28 days splitting tensile strength against stone dust and nylon fiber.

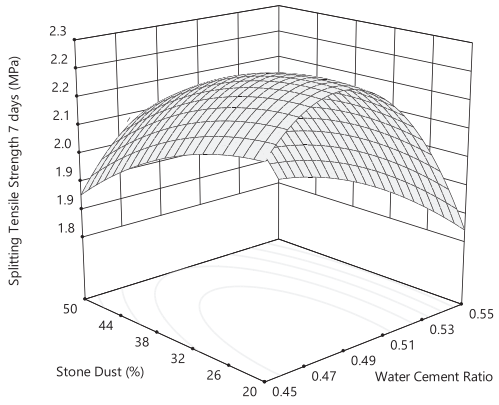


**Figure 19.** Response surface of 7 days splitting tensile strength against stone dust and water cement ratio.

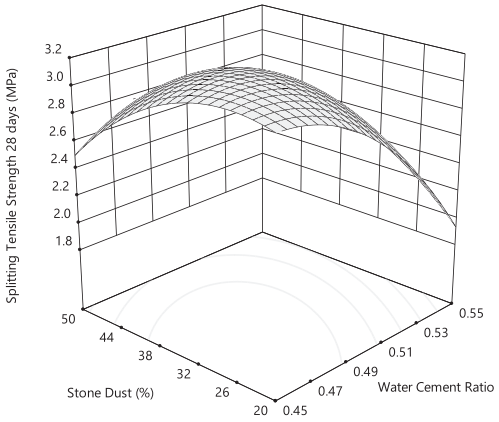


**Figure 20.** Response surface of 28 days splitting tensile strength against stone dust and water cement ratio.

at the mid-level (0.50). Ali et al. (2019) stated that the rise in strength might be due to internal curing and good hydration of cement particles. However, further increment of WC caused decrement of compressive strength that is parallel with the findings of Schulze (1999). Meanwhile, it can be seen from Figure 16 that the strength rises slightly for the increment of NF from 0.25% to 0.50% but decreases markedly when the proportion rises continuously beyond the mid-level (0.50%). Abbas et al. (2002) and Lee et al. (2012) presented similar results in their study. The lowest point of compressive strength was seen at 0.75% NF with 0.55 WC.

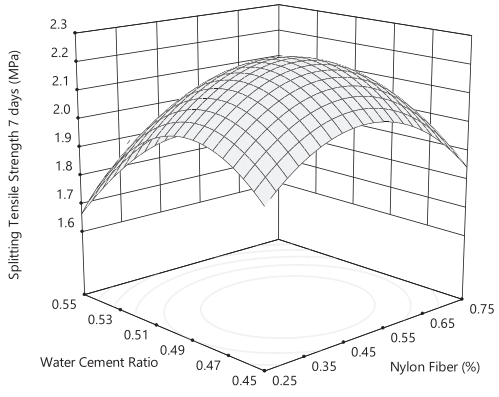


**Figure 21.** Response surface of 7 days splitting tensile strength against water cement ratio and nylon fiber.

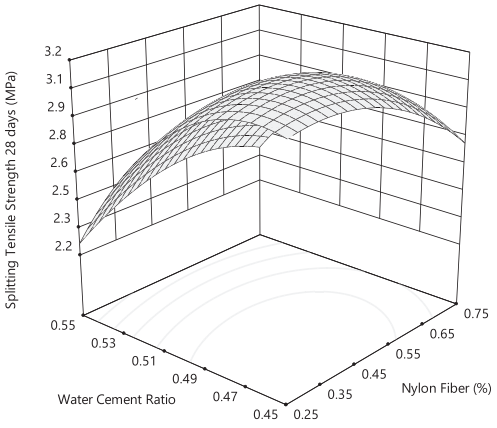


**Figure 22.** Response surface of 28 days splitting tensile strength against water cement ratio and nylon fiber.

### *3.2.2. Splitting tensile strength*

The variations of splitting tensile strength values with SD, NF and WC are presented as response surface graph as shown in Figures 17, 18, 19, 20, 21, and 22. In Figure 17, the maximum value of the strength recorded was 2.17 MPa at 20% SD which matches with the results registered by Joel (2010), Vijayalakshmi et al. (2013). As the content of SD increases, strength decreases to 1.88 MPa identified as the lowest strength occurred at the high level of SD.

It is noticed that, from Figure 17, strength rises with the increase of NF until a certain point (0.50%) and following this percentage strength decreased rapidly with the increasing NF to 0.75%. The excessive inclusion of fiber resulted in porous concrete which reduced the bonding strength between the concrete particles (Ismail et al., 2020). On the other hand, it can be stated from Figure 19 that augmentation of the strength happened from 2.17 MPa at 0.45 WC to 2.22 MPa at 0.50 WC. Peak strength at early ages occurred at 0.5 WC within the range of 20%–50%.

The effects of three factors on 28 days splitting tensile strength were depicted by Figures 18, 20 and 22. It is clear that, from Figure 18, with the gradual rise of SD up to 35% the strength increases which can be attributed to compact matrix caused by fine particles of SD (Khan et al., 2018). Whereas, at the mid-level of NF highest strength occurs followed by an increase of strength from initial level of NF. Lashari et al. (2021) connected the rise of the strength with increased plasticity that delay the initiation of cracks. However, gradual rise in both parameters from the central point caused drop in the strength. For WC, the increment of WC from 0.45 to 0.55 caused the 28-day compressive strength to drop from 3.09 MPa to 1.95 MPA (Figure 22).

## 4. Conclusion

In this research, the effect of incorporating SD as fine aggregate replacement and NF as fiber reinforcement in concrete has been investigated. Also, the influence of water cement ratio on the properties of concrete containing SD and NF has been assessed. Artificial neural network method was employed to develop prediction models for compressive and splitting tensile strength of concrete. Natural sand replacement with 20% and 35% SD generates the maximum compressive strength at 7 and 28 days respectively. Peak compressive strength at early age has been observed at low levels of both SD and NF, however, in later age, peak strength has been gained at mid-levels of SD and NF. On the other hand, splitting tensile strength at early days shows a decline for increasing SD from 20% to 50%, but strength shows an increasing trend for increasing NF (0.25%–0.50%) and WC (0.45–0.5). Splitting tensile strength at 28 days increases with increasing SD and NF up to 35% and 0.5%respectively, whereas decreases for rising WC. All the models developed by ANN were found significant as the statistical values were satisfactory. The simulation capacity of the models was satisfactory due

to the closeness of the predicted results with actual values. However, a detailed investigation can be conducted in future studies in order to observe the physical, mechanical and durability properties of concrete incorporated with stone dust aggregate and nylon fiber.

## Declarations

### *Author contribution statement*

Sourav Ray: Conceived and designed the experiments; Analyzed and interpreted the data; Contributed reagents, materials, analysis tools or data; Wrote the paper.

Mohaiminul Haque: Analyzed and interpreted the data; Contributed reagents, materials, analysis tools or data.

Tanvir Ahmed, Ayesha Ferdous Mita: Analyzed and interpreted the data; Wrote the paper.

Md Hadiuzzaman Saikat, Md Mafus Alom: Performed the experiments; Analyzed and interpreted the data.

### *Funding statement*

This research did not receive any specific grant from funding agencies in the public, commercial, or not-for-profit sectors.

### *Data availability statement*

Data included in article/supplementary material/referenced in article.

### *Declaration of interests statement*

The authors declare no conflict of interest.

### *Additional information*

No additional information is available for this paper.

## References

Abbas, R., El-Rafey, E., El-Shiekh, A., Kamel, A., 2002. Mechanical properties of hybrid fiber reinforced concrete. AEJ - Alexandria Eng. J. 41, 455–464.

Aggarwal, P., Aggarwal, Y., Gupta, S.M., 2007. Effect of bottom ash as replacement of fine aggregates in concrete. Asian J. Civ. Eng. (Building Housing) 8, 49–62.

Ahmad, J., Zaid, O., Aslam, F., Shahzaib, M., Ullah, R., Alabduljabbar, H., Khedher, K.M., 2021. A study on the mechanical characteristics of glass and nylon fiber reinforced peach shell lightweight concrete. Materials (Basel) 14.

Ahmed, A.A.M., Mahzuz, H.M.A., Yusuf, M.A., 2010. Minimizing the Stone Dust through a Sustainable Way : a Case Study of Stone Crushing Industry of Sylhet 215–218.

Akande, O., Owolabi, K.,O., Twaha, S., Olatunji, S.O., 2014. Performance comparison of SVM and ANN in predicting compressive strength of concrete. IOSR J. Comput. Eng. 16, 88–94.

Alawode, O., Idowu, O., 2011. Effects of water-cement ratios on the compressive strength and workability of concrete and lateritic concrete mixes. Pac. J. Sci. 12, 99–105.

Ali, B., Ali, L., Hassan, Q., Baig, S., Malik, S., Din, M., 2019. Effect of molasses and water – cement ratio on properties of recycled aggregate concrete. Arabian J. Sci. Eng. 45 (5).

Alok, G., Ravali, K., Guru Prasad, M., Pravalika, C., Sai Priya, P., Sai Kiran, M., 2020. Strength studies on geopolymer concrete produced by recycled coarse aggregate and quarry stone dust as fine aggregate. IOP Conf. Ser. Mater. Sci. Eng. 981.

Alshihri, M.M., Azmy, A.M., El-Bisy, M.S., 2009. Neural networks for predicting compressive strength of structural light weight concrete. Construct. Build. Mater. 23, 2214–2219.

Anifowose, M.A., Adedokun, S.I., Adebara, S.A., Adeyemi, A.O., Amototo, I.O., Olahan, A.B., Oyeleke, M.O., 2021. Influence of water cement ratios on the optimum use of steel slag in concrete. J. Phys. Conf. Ser. 1874.

Arivumangai, A., 2014. Strength and durability properties of granite powder concrete. J. Civil Eng. Res. 4, 1–6.

Bheel, N., Tafsirojjaman, T., Liu, Y., Awoyera, P., Kumar, A., Keerio, M.A., 2021. Experimental study on engineering properties of cement concrete reinforced with nylon and jute fibers. Buildings 11.

Bisht, K., Ramana, P.V., 2018. Sustainable production of concrete containing discarded beverage glass as fine aggregate. Construct. Build. Mater. 177, 116–124.

Bonagura, M., Nobile, L., 2021. Artificial neural network (ANN) approach for predicting concrete compressive strength by SonReb. SDHM Struct. Durab. Heal. Monit. 15, 125–137.

Choi, S.Y., Park, J.S., Jung, W.T., 2011. A study on the shrinkage control of fiber reinforced concrete pavement. Procedia Eng. 14, 2815–2822.

Dantas, A.T.A., Batista Leite, M., De Jesus Nagahama, K., 2013. Prediction of compressive strength of concrete containing construction and demolition waste using artificial neural networks. Construct. Build. Mater. 38, 717–722.

Demirkir, C., Özsahin, Ş., Aydin, I., Colakoglu, G., 2013. Optimization of some panel manufacturing parameters for the best bonding strength of plywood. Int. J. Adhesion Adhes. 46, 14–20.

Dhir, R.K., de Brito, J., Mangabhai, R., Lye, C.Q., 2017. Production and properties of copper slag. Sustain. Constr. Mater. Copp. Slag 27–86.

Divakar, Y., Manjunath, S., U.A, M., 2012. Experimental investigation on behaviour of concrete with the use of granite fines. Int. J. Adv. Eng. Res. Stud. 1, 84–87.

Duan, Z.H., Kou, S.C., Poon, C.S., 2013. Prediction of compressive strength of recycled aggregate concrete using artificial neural networks. Construct. Build. Mater. 40, 1200–1206.

Gadgihalli, V., Ramya, Shankar, S., Dinakar, R.P., Rani, B., 2017. Analysis of properties of concrete using nylon fiber as fiber reignforcement admixture. Int. J. Res. -GRANTHAALAYAH 5, 63–66.

Galetakis, M., Soultana, A., 2016. A review on the utilisation of quarry and ornamental stone industry fine by-products in the construction sector. Construct. Build. Mater. 102, 769–781.

Getahun, M.A., Shitote, S.M., Abiero Gariy, Z.C., 2018. Artificial neural network based modelling approach for strength prediction of concrete incorporating agricultural and construction wastes. Construct. Build. Mater. 190, 517–525.

Grunwald, S., Frede, H.G., 1999. Using the modified agricultural non-point source pollution model in German watersheds. Catena 37, 319–328.

Gupta, T., Patel, K.A., Siddique, S., Sharma, R.K., Chaudhary, S., 2019. Prediction of mechanical properties of rubberised concrete exposed to elevated temperature using ANN. Meas. J. Int. Meas. Confed. 147, 106870.

Gupta, A., Gupta, N., Saxena, K.K., Goyal, S.K., 2021. Investigation of the mechanical strength of stone dust and ceramic waste based composite. Mater. Today Proc. 44, 29–33.

Hameed, M.S., Sekar, A.S.S., 2009. Properties of green concrete containing quarry rock dust and marble sludge powder as fine aggregate. J. Eng. Appl. Sci. 4, 83–89.

Hammoudi, A., Moussaceb, K., Belebchouche, C., Dahmoune, F., 2019. Comparison of artificial neural network (ANN) and response surface methodology (RSM) prediction in compressive strength of recycled concrete aggregates. Construct. Build. Mater. 209, 425–436.

Haque, M., Ray, S., Mita, A.F., Bhattacharjee, S., Shams, M.J. Bin, 2021. Prediction and optimization of the fresh and hardened properties of concrete containing rice husk ash and glass fiber using response surface methodology. Case Stud. Constr. Mater. 14, e00505. In this issue.

Hassan, W.N.F.W., Ismail, M.A., Lee, H.S., Meddah, M.S., Singh, J.K., Hussin, M.W., Ismail, M., 2020. Mixture optimization of high-strength blended concrete using central composite design. Construct. Build. Mater. 243, 118251.

Ismail, M.H., Rusly, N.S.M., Deraman, R., 2020. Strength and water absorption of concrete containing metakaolin and nylon fiber. Int. J. Sustain. Constr. Eng. Technol. 11, 230–242.

Joel, M., 2010. Use of crushed granite fine as replacement to river sand in concrete production. Leonardo Electron. J. Pract. Technol. 9, 85–96.

Joshi, T., Dave, U., 2016. Evaluation of strength, permeability and void ratio of Pervious concrete with changing W/C ratio and aggregate size. Int. J. Civ. Eng. Technol. 7, 276–284.

Kala, F., Sethuraman, V.S., 2013. Shrinkage properties of HPC using granite powder as fine aggregate. Int. J. Eng. Adv. Technol. 2, 637–643.

Kanojia, A., Jain, S.K., 2017. Performance of coconut shell as coarse aggregate in concrete. Construct. Build. Mater. 140, 150–156.

Kewalramani, M.A., Gupta, R., 2006. Concrete compressive strength prediction using ultrasonic pulse velocity through artificial neural networks. Autom. ConStruct. 15, 374–379.

Khan, A., Nasir, M., Liaqat, N., Ahmed, I., Basit, A., Umar, M., Khan, M.A., 2018. Effect of brick dust on strength and workability of concrete. IOP Conf. Ser. Mater. Sci. Eng. 414.

Khan, M.A., Zafar, A., Farooq, F., Javed, M.F., Alyousef, R., Alabduljabbar, H., Khan, M.I., 2021. Geopolymer concrete compressive strength via artificial neural network, adaptive neuro fuzzy interface system, and gene expression programming with K-fold cross validation. Front. Mater. 8.

Lashari, M.H., Memon, N.A., Memon, M.A., 2021. Effect of using nylon fibers in self compacting concrete (SCC). Civ. Eng. J. 7, 1426–1436.

Lee, G., Han, D., Han, M.C., Han, C.G., Son, H.J., 2012. Combining polypropylene and nylon fibers to optimize fiber addition for spalling protection of high-strength concrete. Construct. Build. Mater. 34, 313–320.

Maran, J.P., 2013. Artificial neural network and response surface methodology modeling in mass transfer parameters predictions during osmotic dehydration of Carica papaya L. Alex. Eng. J. 52, 507–516.

Mashhadban, H., Kutanaei, S.S., Sayarinejad, M.A., 2016. Prediction and modeling of mechanical properties in fiber reinforced self-compacting concrete using particle swarm optimization algorithm and artificial neural network. Construct. Build. Mater. 119, 277–287.

Muhit, I.B., Raihan, M.T., Nuruzzaman, M., 2014. Determination of mortar strength using stone dust as a partially replaced material for cement and sand. Adv. Concr. Constr. 2, 249–259.

Munadrah, M., Irmawaty, R., Muhiddin, A.B., 2021. Study of Self Compacting Concrete performance with addition of nylon fiber. IOP Conf. Ser. Mater. Sci. Eng. 1098, 022013.
Mundra, S., Sindhi, P.R., Chandwani, V., Nagar, R., Agrawal, V., 2016. Crushed rock sand – an economical and ecological alternative to natural sand to optimize concrete mix. Perspect. Sci. 8, 345–347.
Nazerian, M., Kamyabb, M., Shamsianb, M., Dahmardehb, M., Kooshaa, M., 2018. Comparison of response surface methodology (RSM) and artificial neural networks (ANN) towards efficient optimization of flexural properties of gypsum-bonded fiberboards. Cerne 24, 35–47.
Oyekan, G.L., Kamiyo, O.M., 2008. Effect of nigerian rice husk ash on some engineering properties of sandcrete blocks and concrete. Res. J. Appl. Sci. 3 (5), 345–351.
Ozturan, M., Kutlu, B., Ozturan, T., 2008. Comparison of concrete strength prediction techniques with artificial neural network. Build. Res. J. 56, 23–36.
Prakash, K.S, Rao, C.H., 2016. Study on compressive strength of quarry dust as fine aggregate in concrete. Adv. Civ. Eng. 2016.
Prasanth, L., Kumar, K., Syed, A.B., 2020. Study on utilization of zeolite and stone dust in concrete. Int. J. Eng. Technol. Manag. Sci. 4, 93–97.
Rajput, S.P.S., 2018. An Experimental study on crushed stone dust as fine aggregate in cement concrete. Mater. Today Proc. 5, 17540–17547.
Rao, M.C., 2021. Influence of brick dust, stone dust, and recycled fine aggregate on properties of natural and recycled aggregate concrete. Struct. Concr. 22, E105–E120.
Rao, K., Desai, V., Research, D.M.-M., 2012. Experimental investigations on mode II fracture of concrete with crushed granite stone fine aggregate replacing sand. SciELO Bras. 15, 41–50.
Ray, S., Haque, M., Ahmed, T., Nahin, T.T., 2021a. Comparison of artificial neural network (ANN) and response surface methodology (RSM) in predicting the compressive and splitting tensile strength of concrete prepared with glass waste and tin (Sn) can fiber. J. King Saud Univ. - Eng. Sci.
Ray, S., Haque, M., Auni, M.M., Islam, S., 2021b. Analysing properties of concrete made with stone dust and jute fibre using response surface methodology. Int. J. Sustain. Mater. Struct. Syst. 5, 206.
Ray, S., Haque, M., Rahman, M.M., Sakib, M.N., Al Rakib, K., 2021c. Experimental investigation and SVM-based prediction of compressive and splitting tensile strength of ceramic waste aggregate concrete. J. King Saud Univ. - Eng. Sci.
Ray, S., Haque, M., Soumic, S.A., Mita, A.F., Rahman, M.M., Tanmoy, B.B., 2021d. Use of ceramic wastes as aggregates in concrete production: a review. J. Build. Eng. 43, 102567.
Ray, S., Rahman, M., Haque, M., Hasan, M.W., Alam, M.M., 2021e. Performance evaluation of SVM and GBM in predicting compressive and splitting tensile strength of concrete prepared with ceramic waste and nylon fiber. J. King Saud Univ. - Eng. Sci.
Reddy, M.V.S, Seshalalitha, M., Hariprasad, P., 2015. The effect of crushed rock powder and superplasticzer on the fresh and hardened properties of M30 Grade concrete. Int. J. Civ. Struct. Environ. Infrastruct. Eng. Res. Dev. 5, 25–30.
Schober, P., Schwarte, L.A., 2018. Correlation coefficients: appropriate use and interpretation. Anesth. Analg. 126, 1763–1768.
Schulze, J., 1999. Influence of water-cement ratio and cement content on the properties of polymer-modified mortars. Cement Concr. Res. 29, 909–915.
Shariati, M., Mafipour, M.S., Ghahremani, B., Azarhomayun, F., Ahmadi, M., Trung, N.T., Shariati, A., 2020a. A novel hybrid extreme learning machine–grey wolf optimizer (ELM-GWO) model to predict compressive strength of concrete with partial replacements for cement. Eng. Comput. 1–23.
Shariati, M., Mafipour, M.S., Mehrabi, P., Ahmadi, M., Wakil, K., Trung, N.T., Toghroli, A., 2020b. Prediction of concrete strength in presence of furnace slag and fly ash using Hybrid ANN-GA (Artificial Neural Network-Genetic Algorithm). Smart Struct. Syst. 25, 183–195.
Serelis, E., Vitoldas, V., Zymantas, R., Vidas, K., 2018. Waste of granite dust utilization in ultra-light weight concrete. OP Conf. Series: . Mater. Sci. Eng. 442 (1).
Shariati, M., Armaghani, D., Khandelwal, M., 2021. Assessment of longstanding effects of fly ash and silica fume on the compressive strength of concrete using extreme learning machine and artificial neural network. J. Adv. Eng. Comput. 5, 50–74.
Singh, S.B., Munjal, P., Thammishetti, N., 2015. Role of water/cement ratio on strength development of cement mortar. J. Build. Eng. 4, 94–100.
Singh, S., Khan, S., Khandelwal, R., Chugh, A., Nagar, R., 2016. Performance of sustainable concrete containing granite cutting waste. J. Clean. Prod. 119, 86–98.
Srivastava, V., Mehta, Pradeep Kumar, Singh, S.K., Agarwal, V.C., Kumar, R., Mehta, P.K., 2014. An experimental investigation on stone dust as partial replacement of fine aggregate in concrete. J. Acad. Ind. Res. 3, 229–232.
Stathakis, D., 2009. How many hidden layers and nodes? Int. J. Rem. Sens. 30, 2133–2147.
Suman, B.K., Srivastava, V., 2015. Utilization of stone dust as fine aggregate replacement in concrete. J. Multidiscip. Eng. Sci. Technol. 2, 704–708.
Swami, A., Gupta, S., 2016. Use of nylon fiber in concrete. IJSRD-Int. J. Sci. Res. Dev. 4 (5), 2321–613.
Syed, a D.P., Quadri, R., 2013. Effective utilization of crusher dust in concrete using portland pozzolana cement. Int. J. Sci. Res. Publ. 3, 1–10.
Topçu, I.B., Saridemir, M., 2007. Prediction of properties of waste AAC aggregate concrete using artificial neural network. Comput. Mater. Sci. 41, 117–125.
Turuallo, G., Mallisa, H., Rupang, N., 2020. Sustainable development: using stone dust to replace a part of sand in concrete mixture. MATEC Web Conf. 331, 05001.
Vaishnavi, M., Aswathi, A., Sri Saarani, S., Varghese, A., Sathyan, D., Mini, K.M., 2019. Strength and workability characteristics of coir and nylon fiber reinforced self-compacting mortar. Mater. Today Proc. 46, 4696–4701.
Verma, S.K., 2016. Effect on mechanical properties of concrete using. Int. Res J. Eng. Technol. 3, 1751–1755.
Verma, S.K., Singla, C.S., Nadda, G., Kumar, R., 2020. Development of sustainable concrete using silica fume and stone dust. Mater. Today Proc. 32, 882–887.
Vijayalakshmi, M., Sekar, A.S.S., Ganesh Prabhu, G., 2013. Strength and durability properties of concrete made with granite industry waste. Construct. Build. Mater. 46, 1–7.
Wang, K., Shah, S., 2001. Plastic shrinkage cracking in concrete materials—influence of fly ash and fibers. concrete.org. Mater. J. 98, 458–464.
Yadav, R., 2021. Effect of waste glass powder and stone dust on the characteristics of concrete. Int. J. Res. Appl. Sci. Eng. Technol. 9, 421–425.
Yaşar, E., Erdogan, Y., Kiliç, A., 2004. Effect of limestone aggregate type and water-cement ratio on concrete strength. Mater. Lett. 58, 772–777.
Zul, M., Badri, A., Khalid, F.S., Nabil, A., Al, A., Ayob, S., 2021. Performance of concrete containing combination of macro mesh PP and nylon fibers. J. Univ. Tun Hussein Onn Malaysia 2, 475–481.